

FIRST RESULTS FROM THE MULTIBEAM BISTATIC BEAMPARK EXPERIMENTS AT FGAN

Klemens Letsch¹, L. Leushacke¹, J. Rosebrock¹, R. Jehn², H. Krag², and R. Keller³

¹FGAN-Research Institute for High-Frequency Physics and Radar Techniques, 53343 Wachtberg-Werthhoven, Germany

²ESA-ESOC, 64293 Darmstadt, Germany

³Max-Planck-Institut fuer Radioastronomie (MPIfR), 53121 Bonn, Germany

ABSTRACT

In 2006 the first debris observation campaign in the bistatic beampark mode with FGAN's TIRA L-band radar as transmitter/primary receiver and MPIfR's 100 m Effelsberg radio telescope, which was upgraded by a new multi-beam system, as secondary receiver, was conducted. Due to the properties of this high-sensitive 7-beam receiver new algorithms for the estimation of object parameters such as RCS and trajectory were developed which had to work even for sub-centimeter sized objects. As the new algorithms have already been tested with simulated data and partly validated with real data the focus of this paper is their application on the data gathered during the Multi-beampark experiments in 2006 and 2007 and the validation of the results by comparison with the corresponding TIRA data.

Key words: Space debris; Beampark experiment; Bistatic; Multi-beam.

1. INTRODUCTION

The highly dynamic and steadily growing space debris population especially in the LEO region, which is caused by the increasing utilisation of space, requires that statistical debris models such as ESA's MASTER model are validated and updated frequently and regularly. Due to their all-weather and round-the-clock usability high-power radars are the most suitable sensors to perform this task in the LEO range window 250-2000 km.

Since 1993, FGAN with its TIRA L-band radar regularly conducts space debris measurement campaigns, called Beampark experiments, for studying space debris especially in the 1-10 cm object size class. In 1996 these experiments were extended for the first time to a bistatic configuration together with the Effelsberg radio telescope (operated by MPIfR) as a secondary receiver. As both sensor locations are only 21 km from each other the TIRA transmit beam and the Effelsberg receive beam have a large observation volume (see Fig. 1) and the coverage of an altitude area of more than 300 km.

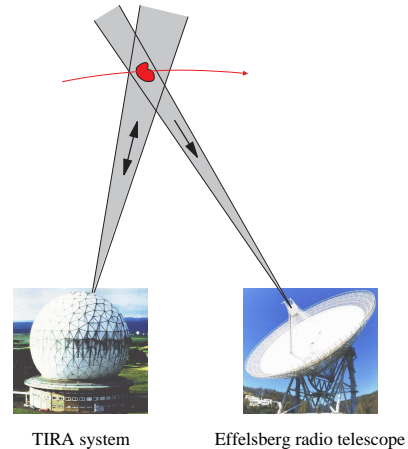


Figure 1. Configuration of the bistatic TIRA/Effelsberg Multi-beampark experiments (MBPE)

The radio telescope's 100 m aperture in combination with cryogenically cooled receivers at a physical temperature below 17 K lowered the detection threshold from 2 cm [3] to 9 mm object size [1] at 1000 km range.

In spite of the improved detection sensitivity of the Effelsberg single-beam receiver a unique RCS and size determination of objects smaller than 5 cm still was not possible because of the unknown beam pattern attenuation and ambiguities caused by the antenna pattern's side lobes. To solve this problem and to enable an unambiguous RCS recalibration the estimation of an object's angular trajectory through the beam is required. Hence, in a cooperation between ESA/ESOC and MPIfR the Effelsberg radio telescope was upgraded by a 7-beam L-band receiver in 2006 (cf. Fig. 2) which should provide a noticeable accuracy improvement for the determination of an object's RCS and its trajectory parameters.

For the generation of object tracks from the acquired multi-beam raw data processing algorithms were used which are quite similar to those applied for the TIRA beampark raw data [3]. However, the multi-beam target analysis and parameter estimation required the development and implementation of new algorithms [6] since the



Figure 2. CAD model of the Effelsberg multi-beam receiver

3dB-single beams of the 7-beam receiver do not overlap as shown in Fig. 3, and therefore prevent the application of the monopulse techniques which are normally used for the determination of the TIRA angular offsets.

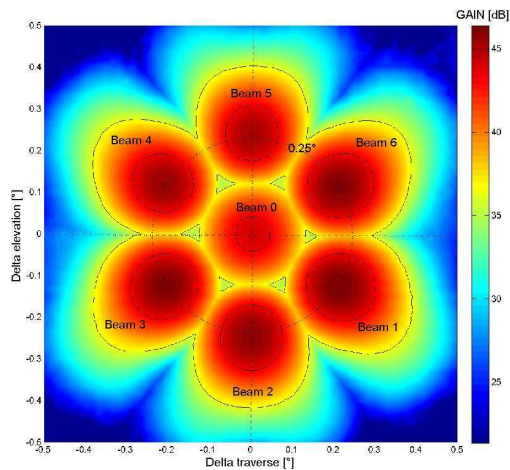


Figure 3. Accumulated antenna pattern of the 7 multi-beam receiver horns

As the new estimation algorithms were already tested with simulated data and partly verified with real data [5] this paper will focus on presenting and comparing detailed analysis results of the processed multi-beam data from the measurement campaigns in 2006 and 2007. The rest of the paper is organized as follows: After a short review of the data processing and analysis chain in section 2 the setups for the Multi-beampark experiments (MBPE) of 2006 and 2007 are given in section 3. In the main section 4 the results of both MBPEs are presented and compared with the corresponding TIRA beampark data. The paper concludes with an overall assessment of the multi-beam approach and its future development and possible improvements.

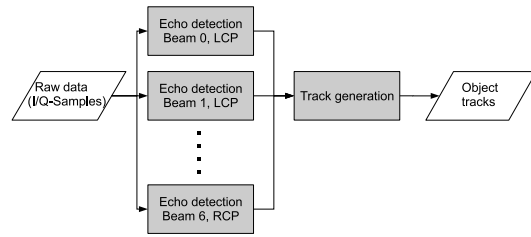


Figure 4. Multi-beampark raw data processing

2. SHORT REVIEW OF DATA PROCESSING AND ANALYSIS

The following section serves as a short summary of the processing stages from the raw data to the results presented in section 4. Detailed descriptions of these stages can be found in [4], [6] and [5].

2.1. Raw data processing

The raw data processing is the most time-consuming stage which is mainly caused by the huge amount of about 3 TByte of raw data for one 24 h observation campaign. According to Fig. 4 the echo detections are determined from the raw data for the 7 beams in principal receive polarization (left circular, LCP) and in addition for the orthogonal polarization (right circular, RCP), too. After performing the steps of coarse matched filtering, threshold detection and fine matched filtering the resulting echo detections are characterized by its detection time, range, Doppler and maximum signal-to-noise ratio (SNR).

Because the typical passage of a LEO object through the beams lasts a few seconds maximum, the same object leads to detections in typically 10-100 consecutive pulses for the chosen pulse repetition intervals of 29-31 ms. Hence, the first task in the track generation stage is to identify detections for each beam which belong to the same object and to sort them into groups. A detection is included into an existing group if its detection time is close enough to those in the group and its range and Doppler value lies within the confidence interval of the corresponding least square estimates of the group.

In the linking step the detection groups from the different beams are associated with each other according to similar criteria used in the grouping step and are stored as object tracks.

Finally, for each echo belonging to a track, information of all channels is selected and written to the track output file which serves as input for the subsequent analysis stage.

2.2. Parameter estimation and data analysis

The data analysis starts with a manual screening (cf. Fig. 5) of each object track to check whether the track parameters show a physically reasonable behaviour and to verify that all detected echos of a track lie within the specified range window and the tracks contain at least 3 detections.

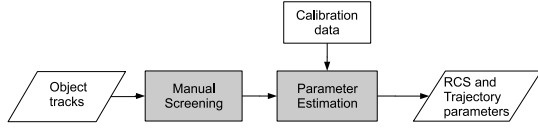


Figure 5. Multi-beampark data analysis

The relevant information about the detected objects include the object radar cross section (RCS) and its trajectory parameters which enable a more accurate RCS determination, but also allows a rough characterization of the object's instantaneous orbital parameters. For the estimation of these parameters from the multi-beam data a parametric approach based on Maximum Likelihood estimation was chosen under the following assumptions:

- The RCS is assumed to be constant during the passage through the beams,
- The majority of detectable debris objects should have a diameter $d < 5$ cm so that the RCS of these small objects at L-band wavelengths is almost independent of the aspect angle and can be calculated using the Raleigh formula [5]:

$$RCS = \frac{9 \cdot \pi \cdot d^6}{4 \cdot \lambda^4}. \quad (1)$$

- Due to the short passage time the trajectory is assumed to be a straight line with constant velocity.
- The echo data are characterized by a poor SNR.

Taking into account the geometry of a MBPE it is appropriate to describe the object trajectory by a parameter vector $\omega = (\Theta, \Phi, \alpha, t_{CPA}, v, R_{CPA})$ consisting of the passage offset angle Θ to the line of sight, the passage direction Φ ($\Phi = 0^\circ$ means north direction) and tilt angle α w.r.t. the plane perpendicular to the Effelsberg antenna axis, the time of closest approach to the line of sight t_{CPA} , the velocity v and the range at CPA R_{CPA} . Applying the radar equation [7] for the bistatic case, the received power P_r^i of each channel i of the multi-beam receiver can be written as

$$\vec{P}_r = a \vec{G}(\omega), \quad (2)$$

with $\vec{P}_r = (P_r^0, \dots, P_r^6)$.

The parameter a only depends on the RCS [6] while $\vec{G}(\omega) = (G^0(\omega), \dots, G^6(\omega))$ contains the trajectory-dependent antenna gains of both sensors, the bistatic ranges and the transmit power.

The measured receive power Y^i of each channel is modelled by the superposition of the noise-free receive amplitudes $\sqrt{P_r^i}$ with a zero-mean complex Gaussian noise which effects both the (I)n phase and the (Q)uadrature amplitude components:

$$Y^i = \left(\sqrt{P_r^i} + n_I^i \right)^2 + \left(n_Q^i \right)^2 \quad (3)$$

where σ^2 denotes the system noise power and n_I^i, n_Q^i are distributed according $N(0, \frac{\sigma^2}{2})$.

The estimation of a and ω requires the maximization of multivariate Likelihood functions [6] which is a non-trivial task since many local maxima of similar height can mislead the search for the global maximum. Therefore a two-step estimation algorithm was chosen which first determines an initial maximum based on an approximation involving Gaussian white noise (GMLE) and then applies a localized search using the more accurate model of Ricean distributed echo data (RMLE). The algorithm was implemented according to Fig. 6 and makes use of genetic algorithms (GA) and the Nelder-Mead simplex method (NM) for optimisation [5].

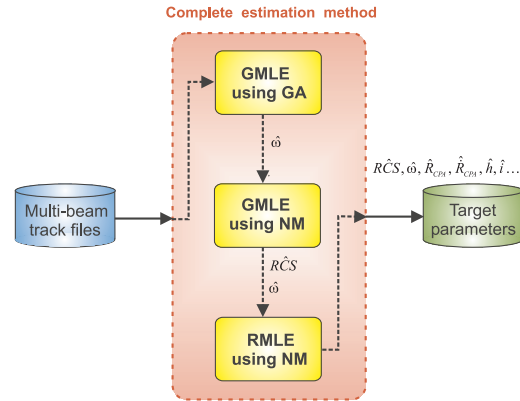


Figure 6. Structure of the implemented estimation algorithm

3. EXPERIMENT SETUPS

The TIRA transmit parameters of the campaign MBPE-1/06 (29-30 Jun 2006) and MBPE-1/07 (22-23 Nov 2007) are listed in tab. 1 and slightly differ in peak power and pulse period. The essential geometry and detection parameters are summarised in tab. 2.

Table 1. Transmit parameters

Campaign	MBPE-1/06	MBPE-1/07
Transmit frequency	1.333 GHz	1.333 GHz
Polarization	RCP	RCP
Peak power	1.3 MW	1.2 MW
Pulse length	1 ms	1 ms
Pulse period	31 ms	29 ms

Table 2. Geometry and detection parameters

Parameter	EFFE	TIRA
Antenna azimuth	90°	93.00°
Antenna elevation	75°	76.12°
Range Window	600-1400 km	300-2000 km
Range Rate Window	±14.1 km/s	±14.1 km/s
NERCS	-63 dBsm	-47 dBsm

A correct determination of the object RCS requires a relative (CAL1) and absolute calibration (CAL2) of TIRA and the Effelsberg multi-beam receiver. For TIRA this is a routine procedure and consists of the insertion of a test signal (CAL1) and the tracking of a spherical calibration satellite. In the case of Effelsberg both calibration steps are realised by measuring the echos from a calibration sphere (in this case TEMPSAT-2) that is illuminated by TIRA and passes through the central beam at a precalculated park position of the Effelsberg antenna. Unfortunately, in the 2007 campaign only the first calibration step could successfully be carried out because the CAL2 raw data recording failed due to an incorrect triggering. Hence, as a preliminary workaround, the calibration factor calculated from MBPE-1/06 data will also be used for the RCS estimation of the objects detected by Effelsberg during MBPE-1/07.

4. RESULTS

During the MBPE-1/07 campaign object tracks were extracted from the receive data of the principal (left circular) polarization because the processing of the right circular polarized echo data is still ongoing. Hence, after completion of processing, the results will be updated if major deviations have occurred from the ones presented within this paper. Tab. 3 gives a quantitative overview of the results for both campaigns and sensors (the column 'Correlated' denotes objects from the TIRA results that could be assigned to catalogued objects). The considerable increase of the detection numbers especially for Effelsberg indicates a rise of the small-size debris population which is analysed more detailed in the next plots. The presentation is organized in 2-plot figures: Within each plot object and trajectory parameters are compared between MBPE-1/06 and MBPE-1/07 whereas the respective upper plot shows the Effelsberg results and the associated lower plot the TIRA results.

Table 3. Number of detections during the Multi-Beampark Experiments 2006 and 2007

Detected objects	EFFE	TIRA	Correlated
MBPE-1/06	424	516	126
MBPE-1/07	738	585	102

4.1. Statistical comparisons

Fig. 7 shows the hourly detection rates vs altitude, divided in 30 km bins. The detection peak for the altitude area 850-950 km in the Effelsberg and TIRA results marks a clear rise of detection numbers between 2006 and 2007 in a known densely populated orbit area. This noticeable increase may mostly be assigned to debris of the former Chinese satellite FENGYUN 1C whose orbit reached an altitude between 850 km and 880 km until its break up in Jan 2007.

Unlike, the small peaks around the altitudes 600 km and 1300 km in the Effelsberg results of 2006 have slightly decreased in 2007 which probably is caused by the revised screening process which discards detections near the edges of the range window. The known peak at 1400 km in the TIRA results has also decreased in 2007, however, the incidents and processes that generate this peak still remain unclear.

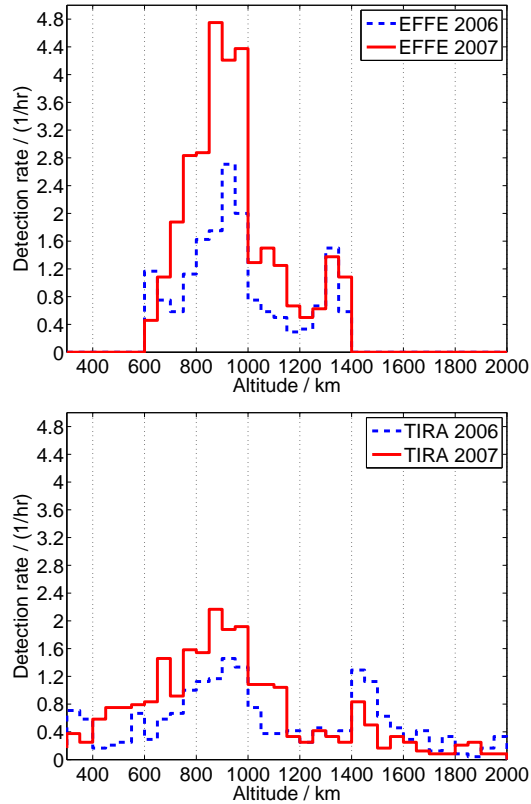


Figure 7. Detection rates vs. altitude, 30 km altitude bins

The hourly detection rates vs. range rate plotted in Fig. 8 show a significantly increased number of detections around -0.5 km/s. Since the inclination is directly determined from the range rate estimations assuming a circular orbit [2], the corresponding peak in Fig. 9 is found around 100 deg inclination. This peak can also be assigned to FENGYUN 1C as this former weather satellite used a sun-synchronous orbit with an inclination of 98.6 deg.

The unusual detections of TIRA around Doppler zero (range rate = 0 km/s) already appeared during earlier beampark campaigns and are under investigation, yet.

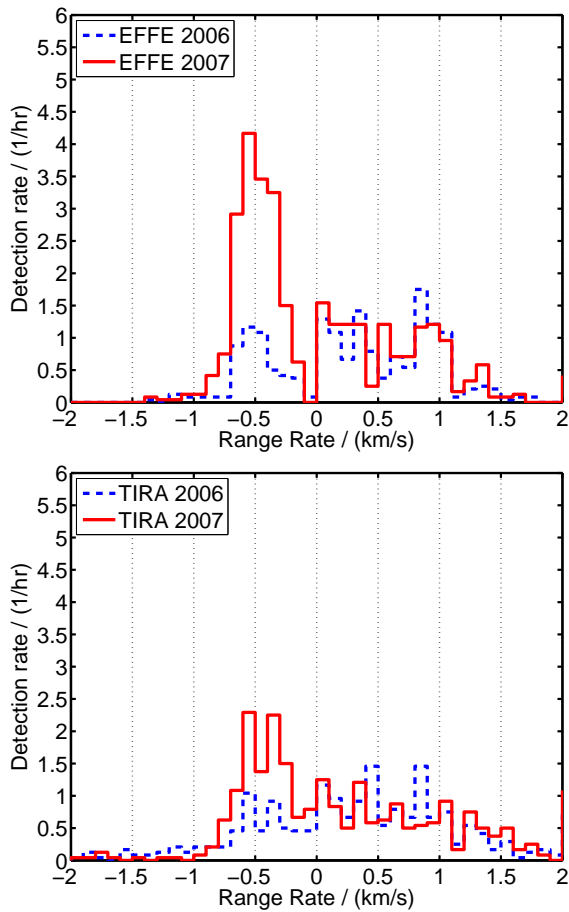


Figure 8. Detection rates vs. range rate, 0.01 km/s range rate bins

Further peaks at inclinations around 82 and 88 deg are visible in the results of 2006/2007 (cf. Fig. 9) and indicate a large and rising number of space debris in densely populated orbit inclinations. On the contrary, the distinct peaks at inclinations around 65 and 70 deg in the results of 2006 seem to have been smoothed in the results of

2007 especially for the Effelsberg data.

Fig. 10 shows the detection rates as a function of object diameter which was determined from the estimated object RCS and NASA's SEM (Size Estimation Model). Besides the known, but still unresolved peak around 4.5 cm in the TIRA plot, a new peak around 2-3 cm has appeared in the results of 2007. This may be an indication that the FENGYUN 1C breakup produced a lot of small debris.

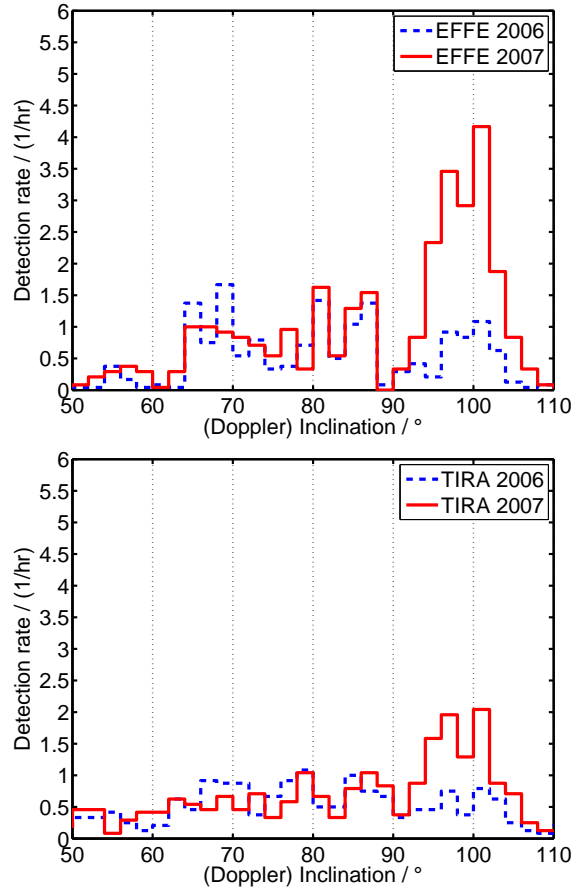


Figure 9. Detection rates vs. (Doppler) inclination, 2 deg inclination bins

4.2. Analysis of the object distributions

The additional scatter plots of the detected objects are helpful for the identification of significant concentrations of objects and the confirmation of conclusions drawn from the histogram plots.

The distribution of the detected objects in the altitude-inclination plane in Fig. 11 shows three object clusterings at an altitude 900 – 950 km and inclinations around 65,

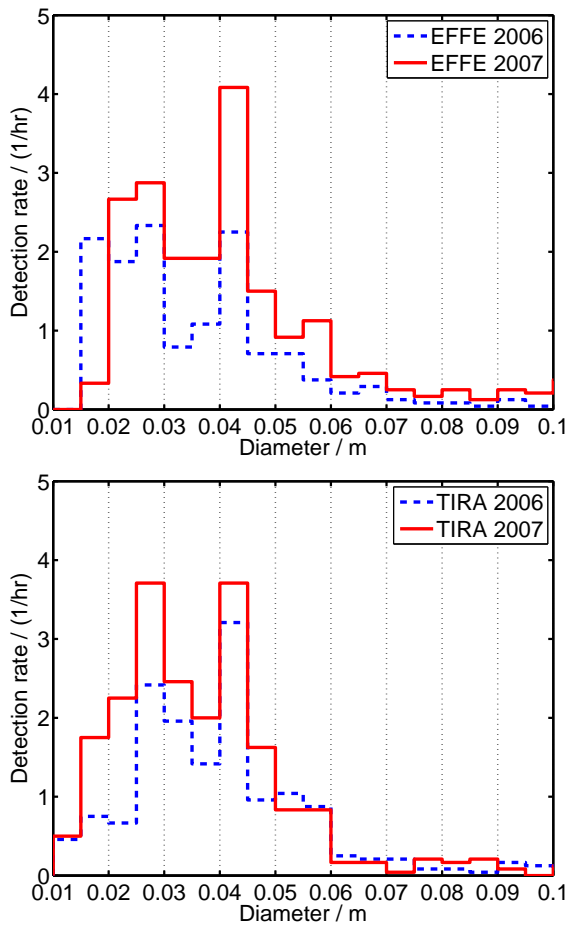


Figure 10. Detection rates vs. diameter, 0.005 m diameter bins

82 and 88 deg which were detected by both sensors in 2006 and 2007. In 2007 a new concentration of objects around an altitude of 900 km and an inclination of 100 deg is clearly visible in the Effelsberg and TIRA plots. This confirms the assumption that the objects of this new cluster are FENGYUN 1C debris.

The dependency between the estimated mean object diameter and altitude is depicted in Fig. 12 where the dashed lines mark the detection thresholds of the respective sensors. The TIRA plot shows a concentration of objects at a diameter of 4.5 cm distributed over an altitude of 800 – 1200 km whereas in the Effelsberg results objects of diameter 2 – 5 cm are concentrated around an altitude of 900 – 1000 km. It should be noted that the Effelsberg plot contains no objects with a size near the detection threshold of the multi-beam receiver. This indicates that the Effelsberg threshold might be slightly higher than expected from theory, but has to be further investigated.

Finally, the scatter plot in Fig. 13 illustrates the dependency between object diameter and inclination and

confirms the already mentioned concentration of objects around an inclination of 100 deg. At this inclination, the distribution of the diameter between 1.8 cm and 6 cm shows no distinct clusterings in the Effelsberg results whereas a concentration at 4.5 cm is visible in the TIRA results which matches with those of the histogram plots in Fig. 10.

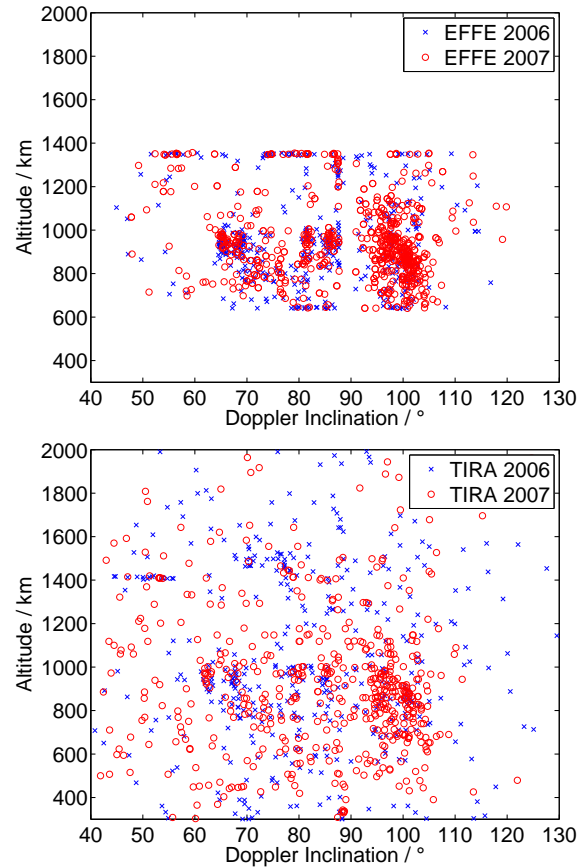


Figure 11. Altitude vs. (Doppler) inclination

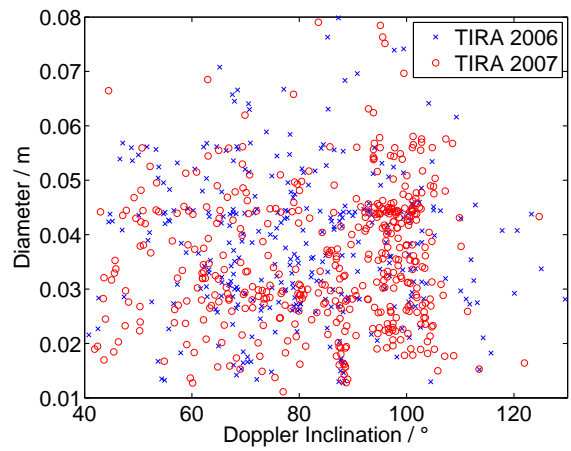
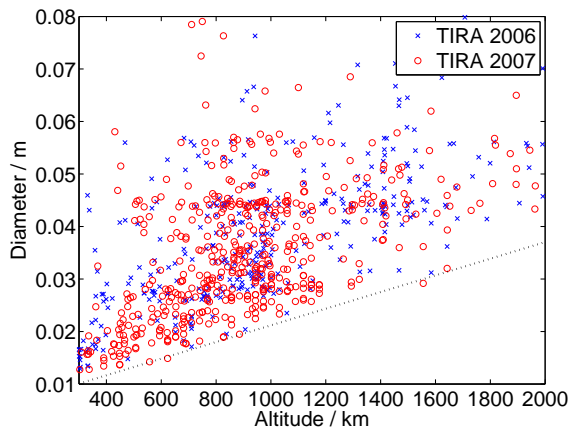
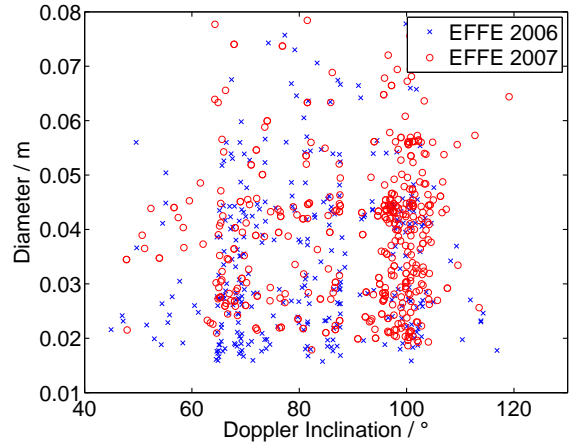
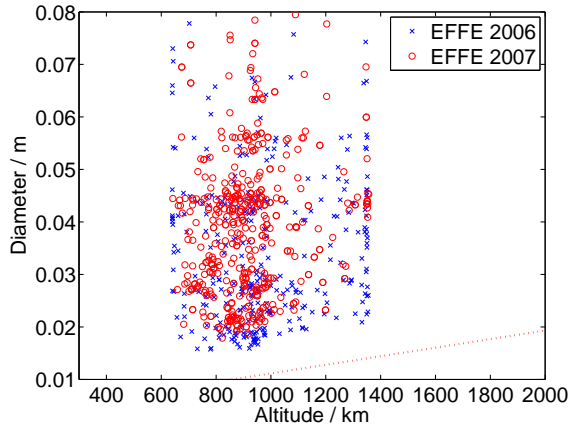


Figure 12. Object diameter vs. altitude

Figure 13. Object diameter vs. (Doppler) inclination

5. CONCLUSIONS AND FUTURE WORK

The presented (preliminary) results of the bistatic multi-beam debris observation campaigns of 2006 and 2007 indicate a general increase of the space debris population caused by continuous activities in space but also confirm a significant increase of objects at an altitude around 900 km and an inclination around 100 deg which can be assigned to the breakup of FENGYUN 1C in Jan 2007. In a next step the obtained results have to be compared with predictions of ESA's MASTER/PROOF model to validate the debris population model.

Besides that, some other work remains to be done to complete the processing and analysis of the MBPE-1/07 data:

- The currently unprocessed RCP data have to be included in the estimation process to consider additional detections and to extract information such as the polarization fraction, necessary for a rough classification of the object's shape.
- The Effelsberg results of MBPE-1/07 have to be cross-checked with the TIRA results and correlated with the parameters of catalogued objects to check their plausibility.
- A detailed analysis is required for object tracks which could not yet clearly be identified.

Concerning multi-beam processing, the results and experiences have shown that the applicability of the new estimation algorithms to real data under the specified assumptions was basically proved.

Nevertheless for raw data processing some modifications and improvements have to be considered since the current offline processing is very time-consuming and tedious. Possible, future modifications may include the optimization of the raw data management and, in the light of today's available computing power, an investigation which parts of the current offline raw data processing could be redesigned and implemented as real-time algorithms.

6. ACKNOWLEDGEMENTS

The authors are very grateful to the colleagues of FGAN-FHR/RWA and MPIfR for the collaboration during the preparation and realisation of the observation campaigns. Special thanks to G. Mueller for carrying out the raw data processing. This work was performed under ESA/ESOC contract no. 17820/03/D/HK/(SC).

REFERENCES

- [1] Leushacke, L., Mehrholz, D., and Jehn, R. (1997). First FGAN/MPIfR Cooperative Debris Observation Campaign: Experiment outline, Analysis Algorithms and first Results. In *Proc. of the 2nd European Conference on Space Debris*, pages 45 – 50, ESA/ESOC, Darmstadt, Germany.
- [2] Leushacke, L., Mehrholz, D., Perkuhn, D., and Peters, H. (1994). Radar detection of mid-size space debris. Final Report of Study Contract 10182/92/D/IM, Darmstadt, Germany.
- [3] Rosebrock, J., Leushacke, L., and Banka, D. (2002). Radar Signal Processing for Space Debris Observation. *Frequenz*, 56.
- [4] Rosebrock, J., Leushacke, L., and Mehrholz, D. (1999). Cooperative debris tracking and development of algorithms for mid-size debris detection with radar. Final Report of Study Contracts 12248/97/D/IM, 12247/97/D/IM, Darmstadt, Germany.
- [5] Ruiz, G., Leushacke, L., Jehn, R., and Keller, R. (2006). Improved FGAN/MPIfR Bi-static Debris Observation Campaign: Experiment outline, Analysis Algorithms and first Results. *57th International Astronautical Congress*, paper IAC-06-B6.1.07, Valencia, Spain.
- [6] Ruiz, G., Leushacke, L., and Rosebrock, J. (2005). Algorithms for multi-beam receiver data analysis. In *Proc. of the 4th European Conference on Space Debris*, pages 89 – 94, ESA/ESOC, Darmstadt, Germany.
- [7] Skolnik, M. I. (2008). *Radar Handbook, 3rd Edition*. McGraw-Hill, New York.